Abstract

Salt marshes are an ecologically valuable coastal habitat under threat from sea-level rise (SLR) imposed by anthropogenic climate change. In recent years, field researchers report finding shallow inundated pools forming on the high salt marshes in New England, causing *Spartina patens* die-back. These die-off pools could be evidence of increased rates of rapid SLR altering the process of high marsh accommodation to sea level, which is well understood under previously slower rates of rapid SLR. However, die-off pool extent and distribution, as well as marsh variables contributing to their formation, are not well documented given how recently they have developed. This thesis explores these variables through a spatial analysis conducted with QGIS on imagery collected and classified via algorithm by the UAS salt marsh research group at the University of Massachusetts Amherst. Raster analyses reveal relationships between bare ground formation and elevation relative to sea level, providing an avenue to validate the probability of inundation in the classification algorithm. This research has important implications for marsh conservation as successful restoration plans rely on updated and accurate information detailing the current state of a marsh. These results also provide an avenue for future research into the factors influencing die-off pool formation, ultimately allowing conservationists to better address this recent development in the impact of SLR on salt marshes. Here, I present the results of an analysis conducted on the Red River marsh in Harwich and Chatham, Massachusetts, to delineate the extent of die-off pools and identify correlative variables.

Introduction

This thesis broadly concerns the effect of sea-level rise (SLR) on salt marshes. Salt marshes are well understood as an ecological hotspot for primary productivity and the proliferation of many ecologically relevant and commercially important wildlife species. This coastal ecosystem is defined by the tidal input of saltwater, which creates a saline environment where halophytic wetland plants thrive and outcompete terrestrial species. The combined impacts of a strong salinity gradient and competition result in the vertical zonation of marsh plants, with species adapted to deep, frequent inundation occupying the low marsh. Saltwater tides reach the high marsh less frequently, where vegetation is not tolerant of deep or frequent inundation.

The hydrologic processes and vegetation community structures that define salt marshes contribute to the functionality of marsh ecosystem services. An ecosystem service is a benefit to the natural environment and humans that exists due to the health of that ecosystem. An example of an ecosystem service salt marshes provide is storm surge protection. A healthy salt marsh with a variety of vegetation can buffer incoming waves by slowing the water velocity as it passes through the marsh, protecting coastal communities and inland ecosystems from storm damage. However, if this marsh suffers from degradation in the form of habitat loss or through other processes that reduce the quantity and diversity of vegetation, it cannot perform this ecosystem service to the same extent. Other marsh ecosystem services include providing nursery habitat for various wildlife, water filtration, and carbon sequestration. Marsh health impacts these services and is often directly compromised by anthropogenic actions such as damming or coastal development. Climate change is readily understood as one of the most

significant impacts humans have on the natural environment, though the exact mechanisms and effects of this process vary by multiple factors in salt marshes.

Researchers have posited many predictions related to the impacts of climate change on marsh ecosystems around the globe. One of the primary effects climate change has on salt marshes is related to sea-level rise. SLR is a result of glacial melting and the expansion of seawater as it warms. As sea levels rise, infrequently flooded areas of the marsh experience greater levels of inundation. The vegetation in these areas is not adapted to deep, frequent flooding stress, resulting in die-back.

Areas of die-back become bare ground; since plant roots no longer trap sediment, erosion rates increase in these spots. Halophytic low marsh species can also colonize die-back patches, but these plants have a lower ecological value on the high marsh due to their reduced functionality as habitat for marsh fauna, making this transition unfavorable. Another impact to marsh functionality imposed by SLR is the reduction of storm surge protection, which is a function of marsh vegetation's capacity to reduce wave velocity. As flooding stress increases in duration and extent, more marsh vegetation is lost, and wave velocity is not reduced as it would be in a healthy marsh. SLR resulting from climate change clearly threatens the resilience of marsh ecosystems and reduces their ability to provide critical ecosystem services.

Salt marshes can compensate for SLR over long periods by migrating landwards as gradual changes in sea level shift the salinity gradient inland. For marshes to compensate horizontally for SLR, there must be undeveloped land adjacent to the marsh for it to occupy as it migrates, and the change in sea level must be gradual over

an extended timeframe. Human action has disrupted this compensatory mechanism by developing coastal infrastructure and increasing the rate of SLR, a direct effect of climate change. These processes in tandem are defined as coastal squeezing since the marsh undergoes habitat loss on the aquatic border and is unable to transgress inland, squeezing the marsh into a smaller area. Marshes can also compensate for SLR through vertical processes that increase elevation; tides and rivers carry sediment to the marsh, where it settles and accumulates. Both horizontal and vertical compensatory processes are influenced by multiple variable abiotic and biotic factors that introduce complexity to modeling these systems.

Addressing and correcting ecosystem degradation requires not only a complete understanding of the system but an effective framework of legislation, policy, and regulation built around this knowledge to facilitate successful, large-scale restoration. While effective to a degree, environmental policy in the United States will only be improved upon when a window of opportunity emerges that motivates action. A policy window opens when an apparent problem is defined, a feasible action to address the problem is brought forward, and sufficient political pressure motivates action. Most legislative and regulatory actions implemented to mitigate the effects of ecosystem degradation occur when the effects of ecosystem degrading processes are visible and a causal relationship between stressor and response can be identified. In other words, clarity surrounding an ecological issue motivates legislative action.

In the case of marsh degradation, decades of research clarify some of the ecosystem impacts related to SLR, though the complexity of this ecosystem hinders this process. Marsh degradation is visible, though its degree of evolution over multiple

decades is not. Furthermore, marsh ecosystems are constantly evolving as energy and material flow through the system, suggesting that any observed change in marsh dynamics could be part of an equilibrating process unrelated to climate change. While there has been much progress in enacting protective wetland legislation in the U.S., gray areas in our understanding of marsh dynamics complicate efforts to propose feasible, effective action to correct or prevent degradation. A solution to these complications could be continuing to collect and analyze data in the hopes that we can open a policy window that effectively addresses marsh degradation caused by climate change.

The unfortunate consequence of waiting for irrefutable evidence before taking action to combat degradation is that potentially less intensive preventative measures are few and far between. Additionally, degradation can, in some cases, sustain itself via feedback loops, indicating that waiting for degradation to occur can increase the risk of permanent damage or reduced ecosystem functionality. These feedback loops are of concern globally, where scientists are trying to predict the timing of climate change tipping points. Identifying the timing of such processes enables us to set management goals and implement policies that reduce the likelihood of reaching tipping points, preventing future degradation. Climate ecologists and similar professionals are managing this same process in the marsh conservation field, where they voice their concerns about the potential feedbacks SLR could alter on salt marshes and how this process could degrade ecosystem services. However, there is not a single feasible action to mitigate these negative impacts due to high levels of variability in ecosystem resilience and factors contributing to vulnerability between marshes. This complicates

our ability to enact both proactive and reactive policies. Furthermore, marsh restoration efforts do not address the root cause of climate change, and solutions to climate change take time to implement and return results. In total, addressing ecosystem degradation related to climate change requires a multifaceted approach whereby implementation of protective and restorative policies reduce the negative impacts of climate change on salt marshes. Research efforts iteratively inform this process through the identification of critical marsh dynamics, which illuminate areas of improvement in the mechanisms of restoration or policy implementation.

Over the last three decades, researchers across many environmental fields published numerous peer-reviewed reports that record their observed impacts of SLR on salt marshes in New England. In most if not all of these papers, the authors emphasize many gaps in knowledge we have yet to clarify related to marsh dynamics. These areas of emphasis currently include marsh-upland boundary dynamics and the effect of vegetation variation on sediment transport and hydrodynamics. These mechanisms are critical when considering the long-term impacts of SLR on salt marshes. While this thesis does not intend to address these areas directly, it will touch upon some of the complexities introduced by the interactions between vegetation and hydrodynamics in understanding present-day marsh response to SLR. More specifically, this analysis explores the intricacy of classifying and interpreting spectral data in a highly heterogeneous and dynamic environment.

Salt marshes are very complex ecosystems with many interacting variables controlling a marshes response to various stressors, making modeling marsh systems in the hope of predicting their response to climate change a difficult endeavor. Predictive

modeling, which utilizes machine learning to forecast the future based on historical response and the current state of the system, is a powerful tool for assessing complex marsh systems. One of the most significant challenges to predictive modeling of marsh response to climate change, aside from existing knowledge gaps related to critical factors, is our inability to base future response on historic response. This challenge arises from the fact that the rate of present-day SLR is significantly greater than it was historically, altering the temporal scale of change in marsh dynamics. Altering this stressor's time scale changes how it impacts the marsh system, which reduces the utility of historical data in predictive marsh modeling. Therefore, developing accurate, informative predictive models relies on identifying and quantifying critical marsh mechanisms, collecting accurate input data, and defining best practices for delineating marsh land cover characteristics.

Many iterations of cumulative effort in developing applicable marsh models have allowed researchers to extrapolate the resilience of marshes under rapid SLR. However, high degrees of uncertainty or conflicting conclusions arise from imperfect input data and model assumptions. For example, different model parameters for sediment availability influence the model's conclusion of overall marsh resilience, where fixed sediment supplies indicate higher resilience (Farron et al. 2020). This discrepancy results from model assumptions related to factors controlling sediment supply, which are necessary due to our incomplete understanding of sediment dynamics. However, technological breakthroughs in recent years expanded our capacity to collect high-resolution data and develop accurate mapping and modeling methodology, introducing avenues to improve predictive modeling. Diligently recording and reporting

observed changes in marsh dynamics as they respond to climate change is crucial as it will help researchers build more accurate models and decrease the uncertainty of their predictions concerning the fate of salt marshes in the coming years.

Improvements to accessibility and functionality of Geographic Information Systems (GIS) represent a significant development in improving landscape-scale analyses. Such spatial analyses are crucial for assessing the state of an ecosystem as a whole, which heavily influences the restoration method and management goals related to that system. With mandatory introductory GIS courses at colleges and universities, students studying environmental science or related disciplines enter the workforce with hard skills developed in landscape analyses that were previously only developed as a specialist skillset. This educational framework encourages further growth in GIS and landscape-scale assessments by promoting system-level thinking and integrating multidisciplinary action into management decisions. GIS established itself as a primary management tool thanks to its ability to conduct large-scale assessments of ecological conditions with relative ease and display results accessibly through mapping, which provides a medium for communication and education. The integration of GIS with other technological advancements only expands upon the utility of this technology in improving our understanding of ecological dynamics and the accuracy of the predictions they inform.

Remote sensing plays a critical role in modern ecological analyses. Beginning in the 1960s and 1970s, remote sensing imagery collected via satellites allowed for global scale classifications of Earth’s surface. In the past ten years, continued technological advancements produced smaller camera systems and sensors fitted to Unoccupied

Aerial Systems (UAS). Concurrent progress in research applications of UAS facilitates collecting small-scale, high-resolution datasets at relatively low cost with high operational flexibility. This allows researchers to access state-of-the-art data collection tools and apply them to the temporal and spatial scales best suited for their studies.

With regard to salt marsh assessments, this is a beneficial attribute of UAS technology since data collected for inundation analyses requires high temporal specificity related to tide cycles. Further growth in this field includes the development of sensors, such as short wave infrared (SWIR) sensors, that expand the spectral absorption features available for analysis, improving the accuracy of vegetation analyses. This sensor and others provide new avenues to conduct landscape-scale assessments based on more accurate metrics of ecological resilience.

Research assessing the condition of salt marshes as SLR progresses, as with many other fields, is a multidisciplinary, multi-step process. It requires the insight of ecologists, hydrologists, climate scientists, spatial analysts, and remote sensing technicians at a minimum. Independent basic research in these disciplines leads to breakthroughs in knowledge and technology that inform the next iteration of collaborative research. This thesis finds itself integrated into this process as it seeks to unite the capability of modern mapping and GIS technology with ecological principles to fine-tune a marsh landcover classification output. The united goal of work done to improve marsh classifications is to provide accurate baseline information related to the current state of salt marshes, which informs both management practices and further research in the world of predictive climate change modeling.

Summary of Work of Previous Researchers

Previous research addressing salt marsh response to sea-level rise (SLR) can be separated into three functional groups:

- Work in identifying marsh dynamics and their response to SLR-induced stressors.
- Work in predicting marsh response to SLR using models.
- Work in improving image analysis, modeling, and mapping.

Each group represents a crucial aspect of understanding and addressing the effects of climate change on salt marshes, though there are various regions of overlap between them. In concert, these research domains work to best inform management and conservation groups in defining the marsh characteristics that reduce their resilience against SLR. This thesis works at the intersection of these groups as it aims to identify marsh response to an SLR-related stressor using image analysis and mapping.

An essential characteristic of salt marsh dynamics relevant to this thesis is their ability to compensate for rising sea levels. SLR compensation occurs through many nonlinear ecogeomorphic feedbacks that increase elevation - vertical processes - or allow the marsh to transgress landward - horizontal processes. In principle, marshes must gain elevation at a rate equal to or greater than that of relative sea-level rise to persist in their exact location over time (Smith 2009, Kirwan and Megonigal 2013, Fagherazzi et al. 2020). Marshes can gain elevation through multiple processes both above and below the marsh surface.

Above ground, sediment deposition plays a vital role in adding elevation to the low marsh. Tidal flooding carries sediment in the water column, which settles onto the inundated marsh, increasing elevation over time. This process implies that low marshes closer to sea level have a greater rate of tidal sediment deposition than low marshes at higher elevations as more of the low marsh experiences flooding (Kirwan and Megonigal 2013). However, this deposition rate is also dependent on the concentration of suspended sediment (SSC) in the tidal column, which is a function of multiple sources - fluvial, oceanic, and erodible (Weston 2014). Dam building and other environmental modifications drastically reduce fluvial sediment supply to marshes, decreasing the rate of elevation gain and, therefore, marsh resilience under rapid SLR conditions (Weston 2014). Plant shoots also contribute to elevation gain by slowing water velocity, allowing particulates to settle and reducing erosion rates. Plants further contribute to elevation gain by supplying organic matter to the surface as they decompose (Kirwan and Megonigal 2013). Evidently, many abiotic, biotic, and anthropogenic factors influence sediment deposition, increasing the complexity of modeling this process.

Below ground, root growth and decay add organic matter to the soil, increasing elevation via sub-surface expansion (Kirwan and Megonigal 2013). Notably, flooding stress impairs below-ground plant growth more so than above-ground growth (Payne et al. 2019). This process implies that as sea levels encroach further up marsh platforms, inundation intolerant species experiencing flooding stress will contribute less to elevation gain through sub-surface expansion than they do currently. However, factors influencing the rate of sediment supply and the contribution of various species to

organic matter production, sub-surface expansion, and sediment transport represent some of the current gaps in knowledge in salt marsh dynamics and response to SLR (Fagherazzi et al. 2020). Nevertheless, these processes represent the base functionality of salt marshes to gain elevation.

Sea-level rise can impact marsh dynamics in a manner that reduces the capacity of the marsh to respond to various stressors, including continued SLR. As previously stated, flooding stress impairs below-ground plant growth across species, implying SLR inhibits a marsh's ability to gain elevation via sub-surface expansion (Payne et al. 2019, Fagherazzi et al. 2020). This dynamic process is particularly problematic in the high marsh, where sediment limited areas gain elevation primarily through sub-surface expansion (Payne et al. 2015). Payne et al. also noted that shoot growth reduces with flooding stress, suggesting SLR could trigger higher erosion rates since less above-ground biomass is available to slow wave velocity. However, tidal flooding can redeposit erodible sediment on the marsh, introducing an avenue to temporarily increasing vertical accretion (Weston 2014). Unfortunately, with higher wave velocity, sediment is not only less likely to settle, but with less plant biomass to trap the sediment, vertical accretion by sediment deposition is reduced at multiple steps in the process (Leonard and Croft 2006).

Furthermore, lower production of plant biomass resulting from flood stress implies that this organic matter input into the soil is smaller, reducing the capacity of vertical accretion and sub-surface expansion to contribute to increasing marsh elevation (Smith 2009). Combining these processes' diminished capacity to increase marsh elevation only elicits more flood stress on the system, creating a dangerous positive

feedback loop (Leonard and Croft 2006, Smith 2009). Flood stress reduces the productivity of marsh plants, which in turn reduces the capacity of multiple mechanisms to increase marsh elevation.

Sediment dynamics represent one of the most significant current gaps in knowledge related to understanding marsh response to SLR (FitzGerald and Hughes 2019, Fagherazzi et al. 2020). However, research establishes that the response of marshes to SLR is highly dependent on sediment availability. Tidal inundation plays a significant role in distributing sediment over a marsh, motivating research into its influence on marsh resilience against SLR. Marshes with the highest deposition rates are low in elevation with a long inundation period, whereas marshes with higher elevations and infrequent flooding have the lowest deposition rates (Kirwan and Megonigal 2013). Longer inundation periods allow more sediment to settle, increasing vertical accretion (FitzGerald and Hughes 2020), though elevation influences the extent of inundation.

Salt marsh dynamics are also heavily influenced by platform elevation and its variation within a marsh system. On average, marshes with a higher mean elevation can resist horizontal compensation for SLR through high marsh retreat, or transgression, while withstanding rising sea levels (Raposa et al. 2017). This relationship indicates that naturally higher marshes and marshes with high accretion rates are resilient against SLR without compensating through landwards transgression. However, the rate of relative SLR is higher than that of elevation gain in 58% of salt marshes in the United States (Cahoon 2015), suggesting that many marsh's responses to SLR will depend on their ability to compensate horizontally by transgressing inland.

In salt marshes undergoing high marsh retreat, steeper elevation gradients correspond to lower rates of vegetation transition from *S. patens*, a non-halophytic species, to halophytic *S. alterniflora* (Smith 2009, Raposa et al. 2017). A marsh may exist on a naturally steep elevation gradient, or it could experience high rates of organic matter deposition on the high marsh. These marsh conditions could be a protective property of such marches in the face of SLR as they can endure higher sea levels with minimal degradation of the high marsh plant community. However, steep elevation gradients inhibit the landward transgression of the marsh-upland border (Raposa et al. 2017). This topographic property could prove problematic if relative SLR exceeds vertical accretion on a marsh unable to compensate horizontally due to a steep elevation gradient. Marshes may also be limited in their ability to transgress inland by coastal infrastructure, including purposeful barriers to marsh migration meant to protect valuable upland property, introducing complexity to the removal of marsh transgression barriers (Fagherazzi et al. 2020). Should such marshes be unable to compensate vertically, they will experience coastal squeeze whereby the marsh area decreases as it erodes or drowns (Langston et al. 2020).

Many decades of research have gone into discerning these ecosystem processes as well as their response to SLR. In 1993, Warren and Niering documented the first observed effect of sea-level rise on southern New England salt marshes. They noted the replacement of *Spartina patens* on a Connecticut high marsh with the more salt-tolerant low marsh species *Spartina alterniflora*. This shift in the high marsh-low marsh vegetation border is a typical initial response of marshes to SLR, especially when sea-level changes over long periods as it has in the past (Smith 2009, Raposa et al.

2017, Fagherazzi et al. 2020). Intuitively, extrapolating the future response of marshes to SLR could be done based on their historic response. However, this method is imperfect due to anthropogenic influence that alters essential (and previously untouched) feedback mechanisms contributing to resilience (Kirwan and Megonigal 2013). The recent acceleration of SLR motivates the development of models that aim to predict the dynamic response of marshes to anthropogenic modification and climate change stressors.

Several widely accepted salt marsh models seek to predict the response of marshes to SLR. Ecological models exist on a continuum of complexity ranging from one-dimensional exploratory models to three-dimensional simulations, offering various levels of utility. The Marsh Equilibrium Model (MEM) is a one-dimensional model that predicts relative SLR and marsh elevation rates for optimizing plant growth and maintaining marsh equilibrium (Morris et al. 2002). In using this model, Morris et al. determined that an optimally productive marsh is more vulnerable to SLR than at lower production levels since optimal production occurs at lower relative elevations. Findings such as these are crucial as they inform marsh managers that optimal productivity should not be set as a restoration goal since it reduces resilience. Various other more complex three-dimensional marsh models have incorporated the MEM as a model component as this field has grown.

Another prominent marsh model, the Sea Level Affecting Marshes Model (SLAMM), predicts the location and timing of any change in inundation resulting from SLR and was one of the first landscape-scale models to incorporate vertical accretion dynamics (Stamp et al. 2019). The most notable numerical models, such as the

SLAMM, are point-based, simulating the complex relationship between inundation frequency and vertical accretion, though sediment deposition rates are simplified as a function of elevation (Langston et al. 2020). However, complex feedbacks between plant productivity, tidal flooding, sediment availability and transport, and the variability of these processes between marshes complicate modeling salt marsh dynamics (Kirwan and Megonigal 2013). Models also inherently carry assumptions that reduce their versatility and increase the uncertainty surrounding their predictions. Despite these assumptions, the SLAMM outputs related to marsh land cover change carry significant implications related to decision-making surrounding marsh restoration priorities.

Modeling to map marsh processes or land cover is a valuable tool for testing hypotheses related to interactions between marsh processes, which elucidates the long-term response and resilience of these ecosystems (Fagherazzi et al. 2012). Several models predict the conversion of New England high marshes to low marsh within the next 100 years (Farron et al. 2020, FitzGerald et al. 2020). Timelines of marsh response to increased SLR scenarios are a critical management tool when considering various courses of action to preserve these ecosystems. Modeling has also shed light on the time lag in marsh response to stressors, suggesting a marsh may take decades to equilibrate after a disturbance (Kirwan and Murray 2007). Without implementing modeling and mapping into research surrounding salt marshes, many crucial breakthroughs in our understanding of marsh dynamics would remain undiscovered.

However, researchers in this field emphasize the need to address multiple underdeveloped domains of knowledge. These include the need to fill gaps in knowledge related to interrelationships between marsh dynamics, the need to collect

more comprehensive data to inform models, and the need to improve model building (FitzGerald and Hughes, 2019, Ganju et al. 2020, FitzGerald et al.,2021). For example, Gustafson (2013) questioned the robustness of predictions based on phenomenological models and suggested mechanistic approaches should be considered when feasible. However, such adjustments to model mechanisms, such as developing a three-dimensional model considering both lateral and vertical marsh processes, require continuous input data that cannot be collected at discrete points in the field (Ganju et al. 2020).

With recent developments in Unoccupied Aerial Systems (UAS) technology, acquiring high spatial and high temporal resolution imagery is more affordable and feasible than in past years (Pashaei et al. 2020). This accessibility, along with developments in algorithm building, opens the door to applying deep convolutional neural networks to marsh land cover mapping, which addresses the challenge imposed by low inter-class variability in salt marshes (Pashaei et al. 2020). Improvements in data collection and processing begin to address some of the challenges inherent to comprehensive marsh analyses: collecting sufficient and accurate data, classifying marsh land cover, and accurately delineating the ecogeomorphic feedbacks that define salt marshes.

Explanation of Current Methodology and Goals

The goals of this thesis are integrated into the larger goals of the research project it assists. This research project, conducted through the University of Massachusetts

Amherst, aims to develop an algorithm that will accurately classify salt marsh land cover characteristics using spectral imagery. In doing so, the research group hopes to develop a technology that can be applied to other marshes and used as a management tool for identifying priority restoration projects and setting monitoring standards. Ideally, this algorithm could be applied to LANDSAT imagery, providing an opportunity to assess marsh conditions on a global scale. While such large-scale analyses have been compiled before, it is necessary to reassess marsh condition both as time passes and as knowledge and technology improve.

More pertinent to this thesis are the goals related to identifying high marsh die-off patches and their relation to elevation, though completing this data exploration also allowed us to explore the algorithm's accuracy. Refining the algorithm is a multi-step process consisting of producing a preliminary classification output, exploring the output and identifying misclassifications, making adjustments to the algorithm, and repeating this process of data exploration and algorithm modification until the desired result is achieved. A salt marsh research team member handles algorithm correction, and thus the suggestions made by this thesis are handed to her and the rest of the team for implementation. This thesis contributes to the algorithm's refinement primarily through data exploration to identify misclassified areas. This research has been ongoing for over three years and will continue well after the completion of this thesis. Therefore, the improvements I suggested during team meetings represent only some preliminary changes to the algorithm and associated methodology before finalization.

One of the primary goals in developing this algorithm is to map inundation accurately. Inundation is a critical variable related to die-off formation, though the exact

relationship remains elusive because of the complex feedbacks inherent to marsh hydrology. As previously mentioned, remote sensing of wetlands presents unique challenges due to the obstruction of inundation by vegetation and the spectrum of soil wetness that sensors cannot differentiate. This implies that while remote sensing can play an important role in delineating the relationship between die-off and inundation, marsh dynamics still complicate this methodology. Since research in wetland spatial analyses emphasizes this challenge as a significant barrier to accurate mapping, this thesis does not anticipate finding a perfect solution. It does, however, seek to suggest a method for delineating inundation using imperfect, though readily available, elevation and tide data.

The other primary goal of this thesis is to identify areas where die-off pools appear to be forming on the high marsh and identify any significance related to elevation, a useful proxy of inundation. A critical attribute of these pools is their shallow depth compared to other potential water features on a marsh. Unfortunately, there is no way to identify the depth of any inundated areas using what data are available. Therefore, die-off pool identification is based on other attributes such as size and location. There are no hard and fast metrics defining what constitutes a die-off pool versus other marsh water features, so this analysis primarily identifies areas that are likely die-off pools.

I completed this analysis using data collected on the Red River marsh. This marsh is in Harwich and Chatham Massachusetts on Cape Cod. The Red River runs through the middle of this marsh, discharging into the Nantucket Sound after passage through a culvert under Deep Hole Road. The study area is roughly 50 acres not

including the upland vegetation or Red River beach captured in some imagery, which are visible in Figure 5 of Appendix A. This marsh is relatively low in elevation with visible ditching scars running off of major water features.

For the entirety of this analysis, I worked off of an orthomosaic image, a Digital Elevation Model (DEM), and two raster outputs from the classification algorithm (see Appendix A). I am working with data from the first rounds of imagery collection done through the spring and summer of 2019/2020. The research team produced the DEM using Agisoft software on spectral data collected via drone. Since vegetation obstruction affects the elevation data, this output DEM is not an accurate measure of marsh surface elevation unless bare ground or water features are visible. This discrepancy is addressed in my analysis through a DEM correction.

The research team used imagery collected at high tide to classify water and bare ground features to avoid mistaking inundated patches for actual bare ground features when they are drained at low tide. They selected this methodology to best capture marsh inundation. Conversely, vegetation was classified using low tide imagery as this guaranteed inundation did not mask flooded vegetation. The group established this methodology after the initial classification, run on a stack of images spanning the entire tidal cycle, misclassified large areas of water/bare ground as vegetation due to mixed spectral signals at these locations. I completed all spatial analyses in Quantum GIS (QGIS), an open-source GIS software.

I based the first method to determine inundation extents solely on the original DEM values calculated using Agisoft. On average, these elevation values overestimate

the actual elevation of the marsh surface, though the degree of overestimation varies by plant species as they grow to different heights. This original DEM, therefore, represents a conservative estimate of inundation extents. To determine ecologically relevant thresholds of elevation corresponding to frequent inundation, I analyzed tide data collected over the calendar year 2020 at Saquatucket Harbor, the closest tide station to the Red River marsh. These data were available through the National Oceanic and Atmospheric Administration's (NOAA) Tides & Currents website.

I began in Excel by calculating three-day running averages, encompassing six high tides each, of the high tide elevations for each month. These data are reported in the NAVD88 datum. I selected the highest high tide 3-day average within each month, representing spring tide levels, and the lowest high tide 3-day average, representing neap tide levels. Next, I calculated the average of all high tide levels over the year to obtain the mean high tide (MHT), which is 0.447m. I then averaged the spring tides and the neap tides from all 12 months to acquire the 2020 annual average spring and neap tide elevations (0.626m and 0.303m, respectively). The MHT acts as a midpoint between the annual average spring and neap tide levels. By finding the midpoint between the annual average spring tide and MHT, I identified the upper bound of frequent inundation that may correspond with die-off formation: 0.536m. Similarly, by finding the midpoint between the annual average neap tide and the MHT, I identified the lower bound of critical inundation extent: 0.375m. These values are tabulated in Appendix B.

I produced a Boolean raster delineating areas on the marsh with elevation values between the critical inundation thresholds using the following expression in the QGIS Raster Calculator:

“DEM@1” <= 0.536 AND “DEM@1” > 0.375

I did so first on the original DEM, producing the layer Original_Inundation, then again on the corrected DEM, producing Delta_Inundation. Doing so allows for a later comparison of the impact applying a corrective elevation factor has on calculated inundation extents and the conclusions one might draw from them. Figure 1 displays these inundation extents over the marsh DEM.

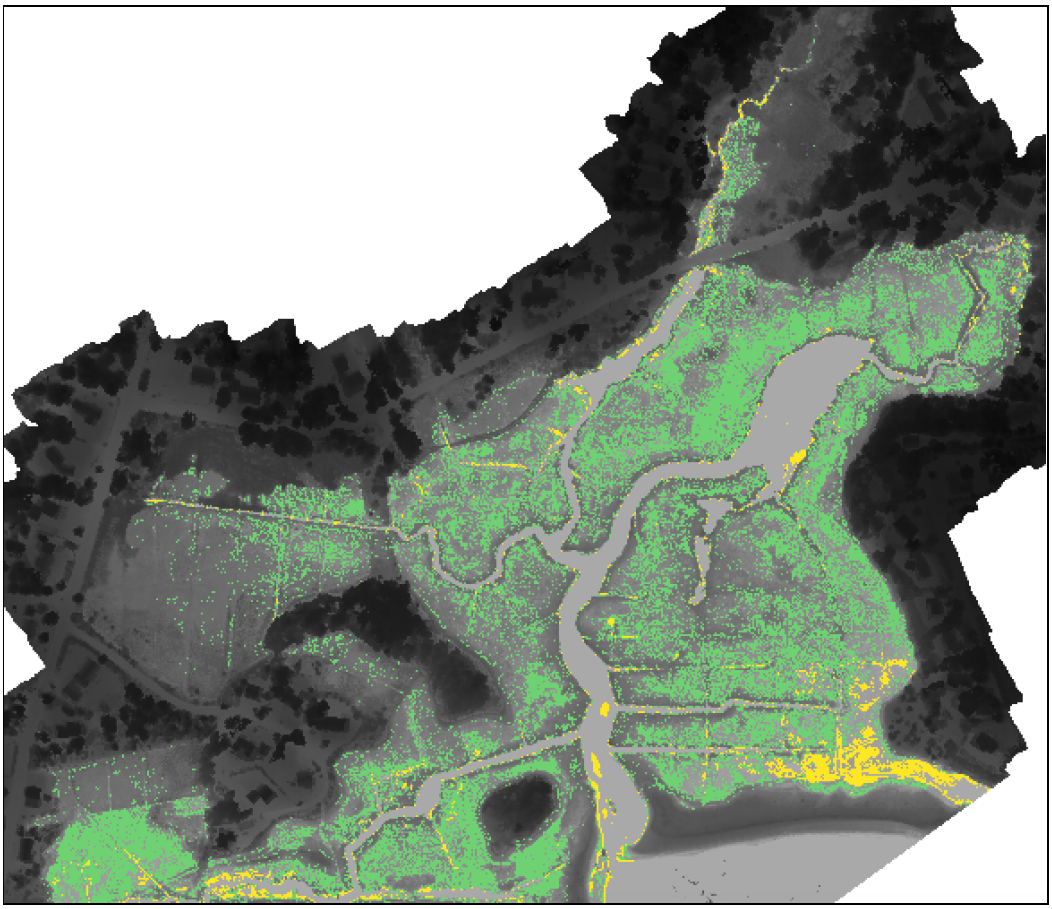

Figure 1: *Critically inundated marsh surface*

Critical inundation corresponds to elevations between 0.375 meters and 0.536 meters. Green pixels represent DeltaDEM derived inundation and yellow pixels represent original DEM derived inundation.

The methodology employed to apply correction factors to the original DEM involved using Real-Time Kinematic (RTK) elevation data. The research group collected ground-truthed elevation values at over 300 points on the Red River marsh in locations that included all vegetation and bare ground classes and one of the water classes. I found the difference between the DEM value and the ground-truthed points at each

sample location using Google Sheets. Next, I calculated the average, median, minimum, and maximum values for the delta values within each class. Not every class was evenly represented during ground-truthing, but most importantly, all of the vegetation subclasses were included. After assessing the range, mean, and median, I determined the median to be the best delta metric for this dataset as they are slightly lower than the mean values on average, reducing the likelihood of overcorrection. These delta values are tabulated in Appendix B.

To subtract the delta values from the DEM in locations corresponding to their respective classes, the vegetation and water/bare ground classification rasters need to be reclassified so that the pixels store their classes' delta value rather than their classification ID number. I did these reclassifications on each raster separately with the Reclassify by Table tool in QGIS. Each class corresponded to a row in the reclass table with the new output values set as the delta value for that class. This tool produced two new rasters holding each class's delta value where that class exists, DeltaVeg (for vegetation subclasses) and DeltaWBG (for water and bare ground classes). Before running this reclassification, I ensured the relevant rasters were displayed in the same projection, NAD83 / UTM zone 19N, and had the same pixel size and extent, ensuring proper alignment. I achieved this result using the Align Rasters tool, where I set the output layers to match the cell size of the vegetation classification raster, preserving these classifications spatially.

After running the Reclassify by Table tool, data inspection revealed that this tool changes the pixel size of the output layer by approximately 3.8×10^{-15} despite no user interaction with this layer property. This pixel size adjustment creates a shift in the data

so that it no longer properly aligns with the DEM, as seen in Appendix A, and it must align for subsequent steps of the DEM correction. To correct this misalignment, I used the Align Rasters tool to align DeltaVeg and DeltaWBG to the previously aligned original VegClasses raster. This method failed to resize the delta raster's pixel sizes properly, so I instead aligned the original DEM, not the previously aligned one, to the delta rasters. Fortunately, this DEM aligned with the delta rasters' cell size and extent. It also held precisely the same elevation values after alignment with the delta rasters as it did when aligned to the original classification rasters.

Next, I subtracted the reclassified vegetation raster, DeltaVeg, from the delta aligned DEM using the Raster Calculator with the expression:

"DEM@1" - "DeltaVeg"

This tool produced a new DEM titled DEM_DeltaVeg. This calculation also changed the pixel size of the output layer, which I corrected via realignment with the DeltaWBG raster extent and pixel size. Since DeltaVeg held 0 values in pixels covering water or bare ground features, the output DEM_DeltaVeg remained unaltered in these areas. This 0 class allowed for the use of the Raster Calculator once more to subtract DeltaWBG from DEM_DeltaVeg using the same syntax as the above expression. The final corrected DEM, DeltaDEM, represents a more accurate interpretation of elevation over the Red River marsh's vegetated areas. As mentioned above, the final step of this second inundation analysis involved using the Raster Calculator to derive the extent of the marsh within the critical inundation threshold range according to the new DeltaDEM.

The final step of this methodology serves to determine the quantitative difference between the inundated area based on the original DEM and the inundated area based on the delta DEM. The inundation rasters must be clipped to the classification extent to obtain relevant percentages of inundation. Clipping required vectorizing a merged raster of the vegetation and water/bare ground classifications, fixing the invalid geometries, and dissolving the resulting polygon to produce a single polygon of the classified extent. The Dissolve tool produced a polygon with holes over pixels with negative values in the classification raster, aptly named MarshExt_wHoles. These negative values result from data transformation during the merging of the two classification rasters, and while this raster no longer holds ecological relevance, the values of these raster pixels are unimportant at this step.

To fill the holes, I created a new polygon shapefile covering the extent of MarshExt_wHoles and subtracted MarshExt_wHoles from the new polygon, leaving polygons in all hole locations. I then deleted the excess polygon to leave the new shapefile layer with only hole polygons and merged this layer with MarshExt_wHoles to produce ClassificationsPolygon. This output served as the mask layer for the Clip Raster by Mask Layer tool, where the input rasters were Original_Inundation and _Delta_Inundation. Finally, I input the two rasters resulting from this clip tool into the Semi-Automatic Classification Plugin (SCP) Classification report tool to retrieve each layer's respective inundated pixel sum versus the total number of pixels covering the marsh.

With the inundation analysis completed, I began the die-off analysis by selecting the major water features on the marsh, namely the Red River itself, to isolate the die-off

features in a separate layer. I did so using the SERVAL, a raster editing plugin for QGIS, selecting the river features with the polygon selection tool and transforming the raster data in this polygon to “nodata.” The output file, DieOffPools, retained all the water and bare ground classified areas not related to the river or ditching activity (Figure 2).

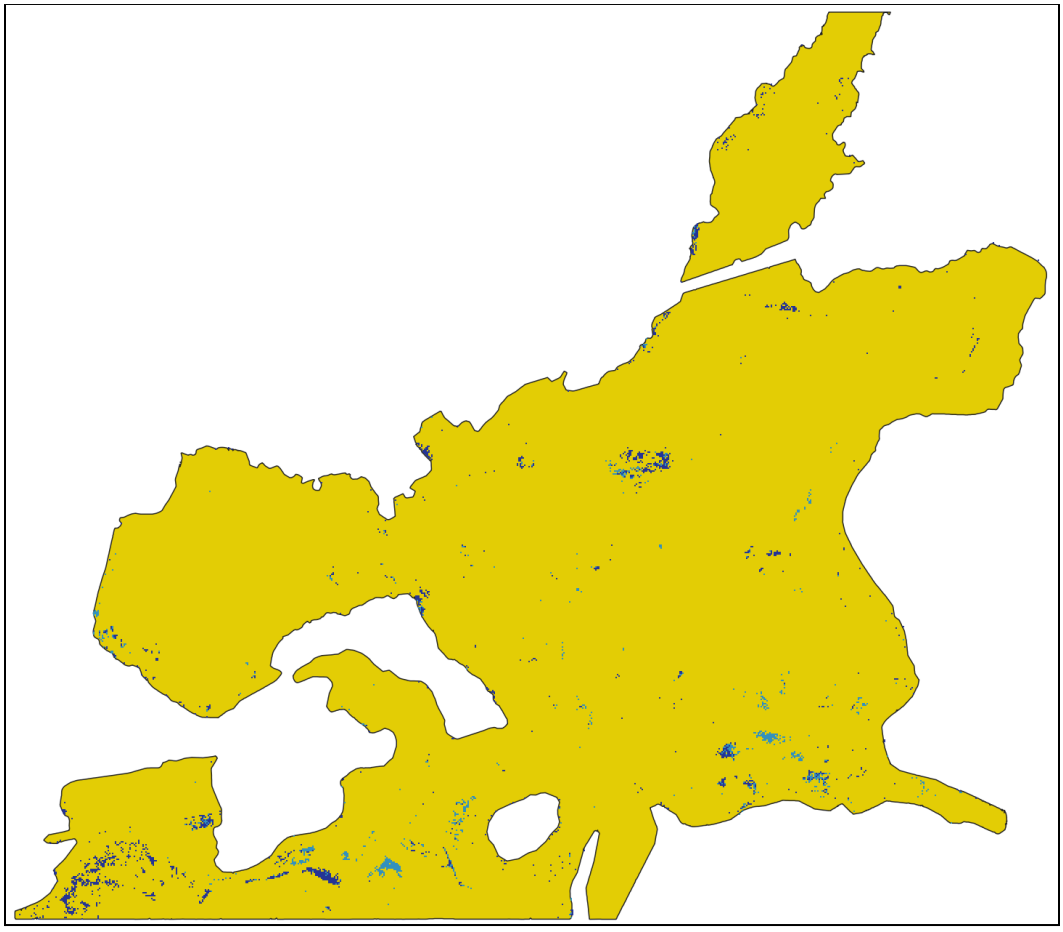

Figure 2: *Die-off pools displayed over the Red River marsh extent*

Not all die-off pools are visible at this scale, though their distribution across the marsh is readily apparent.

To test the significance of elevation contributing to die-off formation, I started by generating random sample points within the die-off features selected in the previous step. This step requires conversion of the pools to shapefiles after removing the 0 class from the DieOffPools raster. I generated 20 random points in this die-off vector using the Random points in layer bounds tool, setting the minimum distance between points to 8 meters. Next, I buffered these points by 5 meters to capture nearby vegetation. To sample the raster below these buffers, I used the Random points in polygon tool to generate 80 random points within each buffer. The target sample size for each buffer is 40 elevation points to reach statistical significance in later analyses.

I oversampled the die-off buffers because some random points are likely to fall on die-off pixels rather than vegetation pixels, and these samples must be dropped. To identify die-off sampled elevations, I erased the DeltaDEM pixels under the die-off vector so that any sampled values here would hold no data, making them easy to spot and erase. Next, I used the Sample raster values tool to extract DeltaDEM values under the 80 points in each buffer and saved the output as a comma-separated values (.csv) file titled DieOffElevs.

To sample elevation in non-die-off locations, I began by buffering the die-off shapefile by 8 meters and dissolving the output to produce a single polygon. I subtracted this output from the ClassificationsPolygon created in an earlier step using the Difference tool to retrieve a shapefile of all areas on the marsh greater than 8 meters away from die-off. I then repeated the methodology used to select sample points in die-off areas, beginning with the generation of 20 random points at least 8 meters away from each other. Then, I buffered these points by 5 meters with 40 random points

generated in each buffer. Since there is no die-off in these areas, I did not have to produce excess points to account for their presence. Once again, I saved the sampled DeltaDEM values as a .csv file titled NonDieOffElevs.

With the sampling data collected, I began the process of data cleaning in RStudio. I used the na.omit() function to remove all NULL values from the DieOffElevs, which occur in sample points generated over die-off. Since this leaves untouched data with nonconsecutive ID numbers, I edited the row names for DieOffElevs, now named dieoff, to clean up the index numbers for the next step using the command: rownames(dieoff) <- 1:nrow(dieoff). I then subsetted dieoff to include just 40 samples for each buffer point by manually calling the row numbers to keep for each buffer point, naming the output dieoff40. This data frame and the nondieoff40 data frame now hold 800 values each, which are evenly distributed across their respective 20 sample locations and are ready to be tested for significant differences in elevation.

This data structure makes it possible to do a repeated measures Analysis of Variance (ANOVA). However, ANOVAs require the data to be normally distributed. I used the Shapiro Test to verify normalcy in both datasets, and neither set as a whole was normally distributed. Since the data violates this assumption, I chose to use the Friedman test, the nonparametric equivalent of the repeated measures ANOVA. This test requires the data to be saved as a matrix, so I saved the elevation columns for dieoff40 and nondieoff40 as variables x and y, respectively, before tabulating these vectors as a matrix with two columns, titled Sample. I then ran the Friedman test on the Sample matrix. I also ran a T-test on the x and y variables despite their violation of normality since this test is still considered robust under normality violations. Finally, I

tested the distribution of these datasets to determine if they came from significantly different distributions using the Kolmogorov-Smirnov test. I also produced a plot of the Empirical Cumulative Distribution Function (EDCF) for both datasets to visualize any differences (Figure 3).

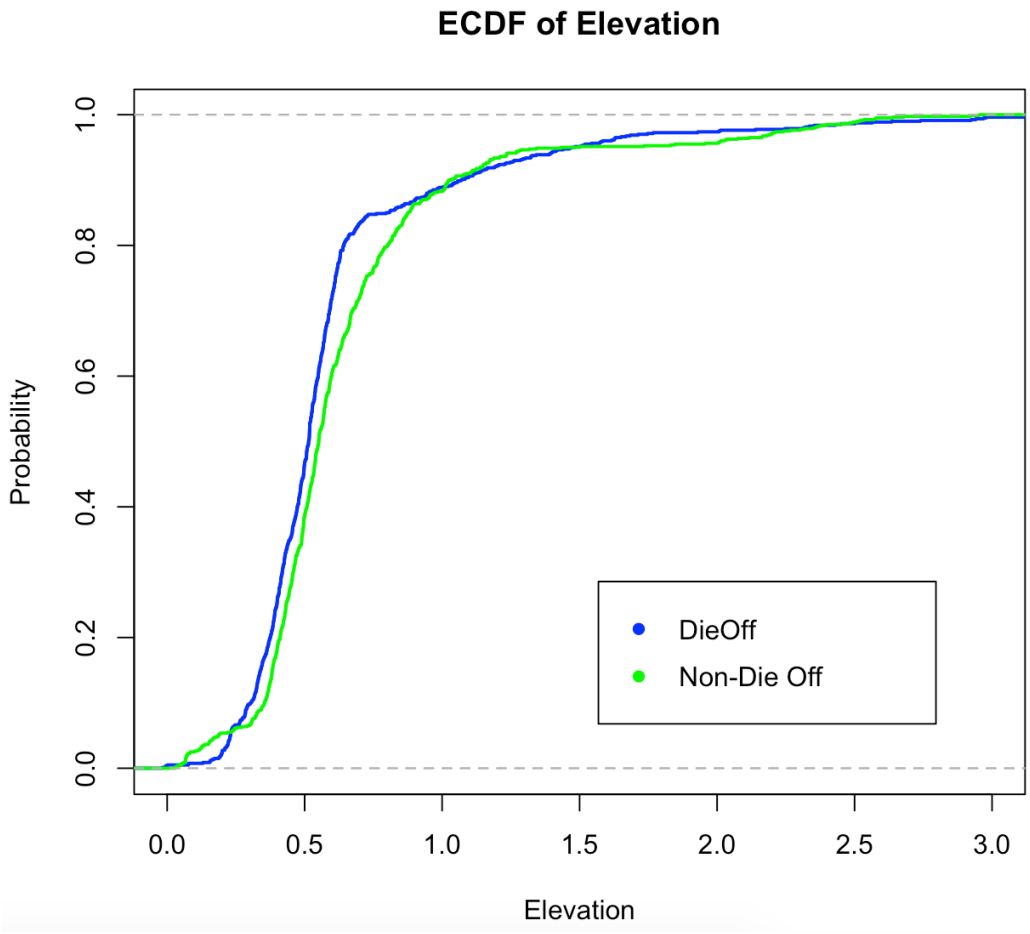

Figure 3: *Empirical CDF for sampled die-off and non-die-off elevations.*

The x-axis shows elevation within the range 0 meters to 3 meters, which encompasses the vast majority of the dataset.

Report and Discussion of Research Results

Inundation Analysis

This inundation analysis first required the identification of ecologically relevant extents of critical inundation. This requires considering oscillations in high tide extents that result from changes in the gravitational pull of the sun and the moon. By calculating a consecutive 3-day running average of high tide levels for each month, I encapsulated the variation of tide heights among months of the year (see Appendix B). The running average for the first five tides of the month required prepending the last five high tides of the previous month to the tide data for the month in question, ensuring all data points were included. Additionally, computing this average on consecutive days preserved the temporal frequency of inundation levels, which is crucial to consider as the frequency of flooding impacts plant resilience. Variance among spring and neap tides is low (0.00187, 0.00184, respectively). The lowest spring tide running average occurred in January at 0.5517 meters, which is 0.208 meters higher than the highest neap tide running average in May at 0.3467 meters. A paired two-sample t-test confirmed that the spring tide averages are significantly greater than the neap tide averages (P = 5.079x10-11).

The inundation analysis resulted in the output of two Boolean rasters delineating the extent of critical inundation on the marsh. The first inundation raster, OriginalDEM_Inundation, is derived from the original DEM's elevation values. The second inundation raster, DeltaDEM_Inundation, is derived from the elevation values held in the DeltaDEM raster. Both rasters select elevation values within the range of

0.373 meters to 0.536 meters. The original DEM reports 2.68% of the marsh as critically inundated, while the delta DEM reports 25.7% of the marsh as critically inundated (Figure 1). I obtained these values through the SCP Classification report for each inundated layer. This increase in inundation extent after DEM correction suggests 23.02% more of the marsh platform is susceptible to die-off formation than was reported by the original DEM. Such a difference proves the necessity of carefully considering ecological properties such as plant height when determining the accuracy of raw DEM data.

While the application of a delta value by vegetation subclass and water/bare ground classes to the DEM successfully reported a more plausible inundation extent, it is crucial to consider the limitations of this method. For example, this method does not account for intraspecies variation in plant height. A variance analysis of the delta values derived from each ground-truthed elevation point reveals a range of variances associated with each subclass, though all variances are less than 0.2, indicating low variance overall. Vegetation subclass 12, representing *Phragmites*, held the highest variance at 0.127. This variance could result from *Phragmites* invasion, where variation in plant height could reflect various stages of *Phragmites* succession as suitable saline habitat develops. The lowest variance, 0.002, belongs to the species *Juncus gerardii*, a high marsh species.

It is important to consider the data's sample size when interpreting variance. As a statistical rule of thumb, sample sizes <5% of the population size are considered unreliable. We can consider the population size for each subclass as the number of pixels it covers and the sample size as the number of ground-truthed points used to

derive the delta value for that subclass. Each vegetation subclass has a population size on the order of 100,000 to 1,000,000, meaning a 5% sample size of even the smallest subclass populations consists of 5,000 RTK measurements. Since I was working with roughly 330 RTK points total, none of the calculated variances are reliable. Therefore, I cannot accurately assess the variation among subclasses to determine if multiple delta values for each species dependent on geographic location, such as proximity to water features, would further refine the DEM correction. Theoretically, identifying spatial relationships between plant height variation within a species would offer an avenue for empirical refinement, though the degree to which this would alter resulting critical inundation extents is unknown.

Die-Off Analysis

This analysis required the manual extraction of die-off features using the QGIS SERVAL plugin. An alternative method such as selecting features of a specific size through a cluster analysis could have potentially missed larger interconnected clusters of die-off. With this in mind, I determined manual selection to be the best available method of die-off extraction from the larger joint water/bare ground classified raster as it provided control over the high variability in water/bare ground features. I found that die-off features comprise 1.46% of the marsh. This percent cover could be a promising result since the inundation analysis revealed that 25.7% of the marsh is critically inundated and likely vulnerable to die-off formation.

Furthermore, just 33% of the pixels comprising die-off patches fell within the critical inundation range. These ratios could suggest that the die-off patch development

is a function of more variables than solely inundation level, implying we can promote marsh resilience through means other than reducing inundation. These other variables may include vegetation species and diversity or nutrient availability. Despite our previous knowledge that marsh processes are multiply determined, these findings are hard lines of evidence supporting that claim.

However, this die-off selection method has some limitations of its own related to user discretion. There were multiple “edge cases,” as I defined them, where it was difficult to discern if a water feature near the river or ditching channels was a continuation of that feature or if it arose due to favorable die-off conditions (Figure 4). I attempted to base my decision on as many ecological context clues as possible to reduce the likelihood of misselection. For these edge cases, I referenced the orthomosaic image of the marsh to provide more visual indicators of either die-off presence or channel features. For example, some small patches classified as water near the river channel are connected to the river system via a small channel obscured by vegetation. These channels are occasionally misclassified as vegetation, allowing mistaking these pools as die-off features. Upon inspection of the orthomosaic image in such areas, it is clear these features directly connect to the river and represent a separate ecological process contributing to pool formation. I also considered the proximity to actual die-off patches since proximity serves as a proxy for identifying the presence of favorable die-off conditions. Finally, any strictly linear clusters of water/bare ground pixels were not included as die-off features as they likely represent ditches despite their visual similarity to true die-off.

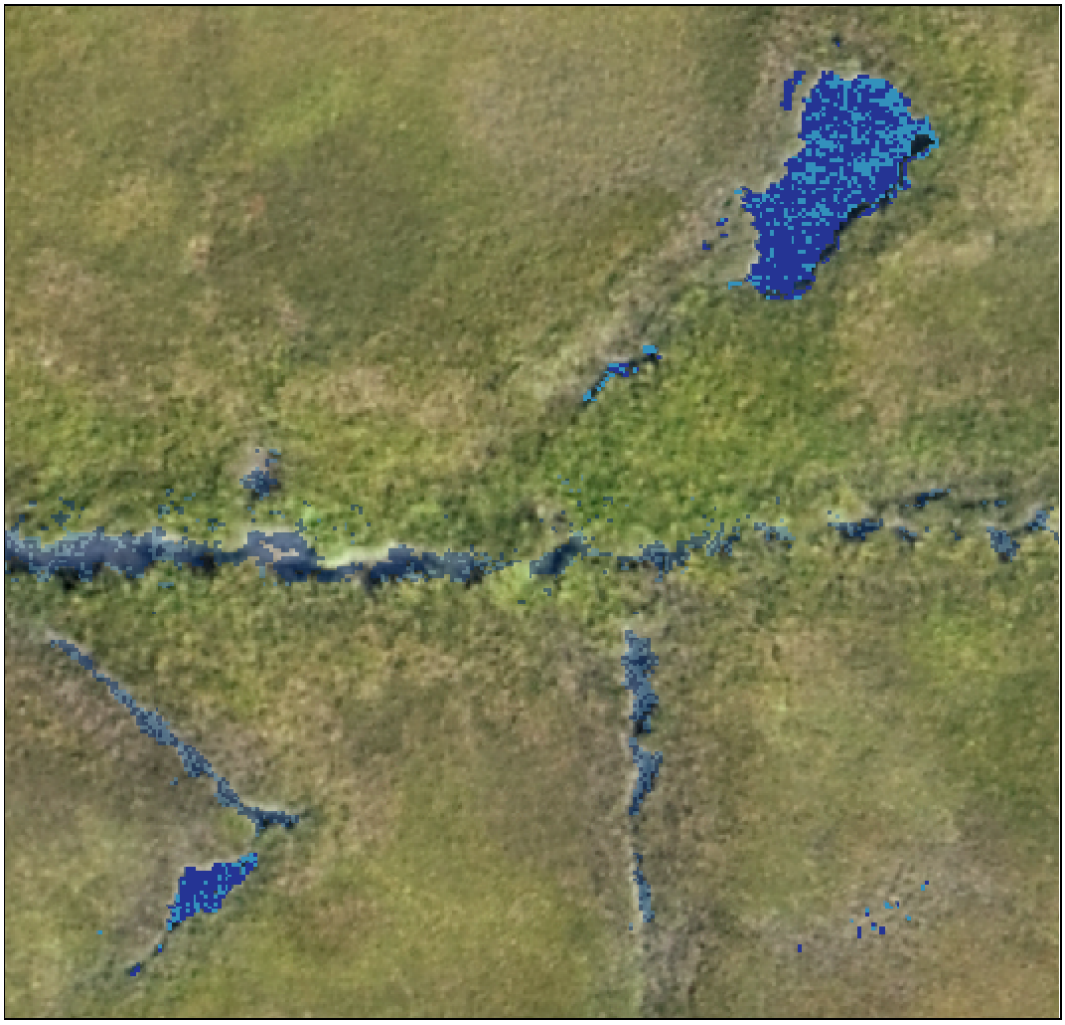

Figure 4: *Example of die-off edge cases*

In this image, it is unclear whether the opaque blue pools arose because of their proximity to a ditch (running through the center of the image) or if SLR-driven processes resulted in their formation.

The analysis I conducted in RStudio to determine a significant difference in elevation surrounding die-off compared to marsh areas without die-off revealed no significant difference in elevation between these two conditions. For reference, the mean die-off elevation is 0.61580 meters and the mean non-die-off elevation is 0.65937

meters. The *P* values returned by the Friedman test and the t-test, which support this conclusion of insignificance, were *P*=0.08969 and *P*=0.05781, respectively. Neither *P*-value falls below the 0.05 confidence level, meaning neither null hypothesis can be rejected with 95% confidence. For the Friedman test, the null hypothesis states that there is no significant difference between the two treatments, die-off presence versus die-off absence. The t-test null hypothesis states that the difference in means between the two groups is equal to zero, indicating no difference. It is worth mentioning that these results could be accepted as significant under a lower confidence level, though it is important to consider reasons for not rejecting the null hypotheses at 95% confidence. These tests suggest elevation does not play a role in determining the presence of die-off, though their null hypotheses do not test for all possible variation among data.

Given the lack of statistical significance in the difference between die-off and non-die-off elevations, the result of the Kolmogorov-Smirnov test was unexpected. The resulting P-value from the two-sided version of this test was well below the 0.05 significance level at *P*=4.107e-08. This result allows us to accept the alternative hypothesis that these data come from different distributions. A one-tailed version of this test also returned a P-value below 0.05 (P=2.053e-08), allowing us to accept the alternative hypothesis that the non-die-off Cumulative Distribution Function (CDF) falls below the die-off CDF.

To interpret this result, I referenced the empirical CDF plot of both datasets (Figure 3). It appears that the largest difference between ECDFs occurs just below 1 meter in elevation, where there is approximately an 80% chance that you will randomly

sample a non-die-off elevation less than or equal to *slightly below* 1 meter. In contrast, there is an 80% chance that you will randomly sample an elevation less than or equal to *well below* 1 meter around die-off. Essentially, at most probabilities over this distribution function, there is a statistically significant chance that one samples a slightly higher elevation in non-die-off areas than in die-off areas, though this difference is greater at elevations just below 1 meter and around 0.25 meters. This difference makes sense ecologically as we expect lower elevations to contribute to die-off formation. Despite the failure to reject the Friedman and t-test null hypotheses stating zero difference between the treatments/mean elevation values for die-off and non-die-off areas, the Kolmogorov-Smirnov test reveals that die-off pools can affect the distribution of randomly sampled elevation points.

It is necessary to acknowledge the limitations of this sampling approach in identifying a relationship between die-off and elevation. The primary limitation derives from failure to exclude areas of the marsh with unique elevation dynamics resulting from variation in sediment accretion rates across the marsh. The inundation analysis revealed that most riverbank and runnel channel edges are not critically inundated despite their proximity to open water. While this may seem counterintuitive, it is a well-studied effect of spillover sediment accumulating on river channel edges or spoil piles around ditching. However, die-off still occurs close to these sediment piles. This means random sampling of such die-off pool vegetation could be extracting elevation values on these piles, which misrepresent the elevation of vegetation directly surrounding die-off. This analysis did not directly consider the impact of variation in sedimentation rates on marsh surfaces, though I suggest similar future analyses should

intend to do so. One method for improving vegetation selection could be to reduce the 5-meter radius for buffering the random sample points to concentrate samples closer to die-off edges, though such a correction would result in a higher percent of sample points generating on die-off pixels.

Furthermore, my sampling method assigned equal weight to all sample locations despite the variety of die-off characteristics they represent. Some die-off pools are multi-pixel clusters with visible water on the orthomosaic image, while others are comprised of one to a few pixels with few visual clues to confirm die-off. Assuming all die-off is accurately classified, this variety likely represents multiple stages of die-off progression that may relate to elevation in various degrees. It could be useful to re-conduct this sampling analysis on die-off pools of similar size and structure to reduce other variable interactions, such as die-off size. Alternatively, rasters calculated by the salt marsh research team display the probability of inundation over the marsh and could have been used to select die-off locations with high inundation probabilities. However, this method could introduce a sampling bias based on the assumption that die-off occurs in high inundation probability locations, so such a methodology should be cautious and base its decisions on sound ecological principles. In any case, I emphasize the importance of future research eliciting identification features for die-off that increase our certainty of their selection.

Additionally, since the classification algorithm has not yet reached its final, most accurate version, we recognize that the outputs I used likely misclassified some of the pixels sampled for buffering. These potential misclassifications would mean that some sample points could be based around “die-off” that is not truly present in that location,

meaning they misrepresent the elevation around actual die-off patches. A more accurate representation of die-off elevation could result if this analysis more heavily weighted the elevations surrounding sample locations with a high probability of die-off. However, this method is also subject to sampling bias, and thus I continue to emphasize the importance of identifying proper die-off selection attributes to preserve statistical power in their analysis.

Conclusions and Implications for Future Research

While salt marshes can compensate for natural rates of sea-level fluctuation, anthropogenic climate change has increased the rate of sea-level rise over a temporal scale that reduces the efficacy of these processes in promoting marsh resilience. Features such as die-off pools develop due to rising tides that rapidly change the inundation stress defining marsh plant community structure. These die-off pools reduce the capacity of a marsh to provide critical ecosystem services. This reduction in function motivates research projects such as this thesis to map the extent of die-off, ultimately providing an avenue to assess the current state of die-off development.

Overall, we can conclude that the Red River marsh is experiencing die-off, though this analysis could not define a causal link to inundation stress related to SLR. The spatial analysis found that 1.46% of the Red River marsh surface consists of die-off. Comparatively, 25.7% of the marsh surface is critically inundated, where critical inundation corresponds to elevations between 0.375 meters and 0.536 meters. The DEM correction reported a nearly 860% increase in the percent of critically inundated

marsh surface compared to the original DEM, from 2.68% to 25.7%. A statistical analysis testing for a significant relationship between die-off and elevation reveals no mean difference between elevation samples taken around die-off and far from die-off. However, the distribution of elevation values for these two variables is statistically significant, with the ECDF for die-off elevations falling above the ECDF for non-die-off elevations. This result implies a higher probability of sampling a higher elevation value in non-die-off vegetation compared to vegetation near die-off.

There are areas of improvement within this thesis that could result in higher quality DEM production. It was clear after producing DeltaDEM that this raster, despite representing smooth elevation data, became polygonized and reminiscent of the vegetation raster classification boundaries in some areas. I suggest future corrections of DEMs with this method should seek to integrate a smoothing factor to account for transitions from one class to another. Furthermore, spatial variation in intraspecies plant height was not considered in my methodology, though this adjustment could also improve DEM accuracy by applying delta values unique to specific patches of vegetation subclasses.

Due to the proximity of the Friedman test and t-test *P*-values to the 0.05 value for significance, I suspect improvement of my die-off elevation selection may shift this result past the significance threshold. I base this conclusion on the results of the Kolmogorov-Smirnov test that imply a fundamental difference in the distribution of elevation values around die-off and far from it. This could be achieved by altering the buffer distance, increasing sample size, and increasing the stringency of die-off

selection criteria. Adjusting these parameters may reveal a relationship between these variables that isn't apparent under my current sampling methodology.

The reduction of ecosystem service functionality resulting from die-off motivates the implementation of targeted management strategies and continued research related to understanding marsh dynamics. Both effective management and rigorous scientific research require accurate, detailed baseline data that allows for the development of evidence-based conclusions. Technological advancements in remote sensing and spatial analyses that increase the depth and computational power of ecological analyses support the generation of reliable data.

The application of UAS technology to ecological remote sensing expands our capacity to acquire data with high temporal and spatial resolutions by cost-effective means. UAS, including drones, offer a high level of user preference related to the flight time of day and collection frequency that are not accessible when using data from satellites. Control over temporal frequency is of particular importance in the remote sensing of tidal ecosystems such as salt marshes, where it is necessary to consider the desired tide level during imagery collection. In a similar vein, controlling temporal frequency also allows for selecting ideal flight dates, which might consider the timing of growing seasons or weather conditions. Command of these variables promotes the acquisition of maximally useful data.

This principle of control over the temporal frequency of imaging benefitted the development of the salt marsh research group's classification algorithm. Initially, the team produced a classification raster of vegetation, water, and bare ground classes

using a stack of orthomosaic images from various stages of the tide cycle. This classification misclassified open water as low marsh vegetation in some areas. However, data inspection revealed this was likely a result of the input imagery structure, not the algorithm itself. To avoid these misclassifications, vegetation must be mapped at low tide separately from water and bare ground, which are mapped at high tide. Since the group already acquired imagery at all desired tidal heights, they could rerun the classification with a new, two-part methodology; classify vegetation using low tide imagery and classify water and bare ground using high tide imagery. Were it not for their ability to preemptively select ecologically relevant snapshots of the marsh and time their flights accordingly, the correction of these misclassifications would have required more time, energy, and resources than it did with conscientious drone data collection.

Another impressive quality of UAS remote sensing is the high spatial resolution it provides. Compared to satellite sensors, which collect data at a resolution anywhere from 1 meter to 500 meters, the drone data acquired for this project was collected at an 8-centimeter x 8-centimeter resolution. This drastic increase in resolution allows for the development of a more spatially refined marsh land cover classification. This refinement provides a more accurate representation of marsh characteristics that is useful in informing management decisions related to specific marsh dynamics.

In the context of this thesis, high spatial resolution is a critical data attribute as the algorithm could detect even the smallest die-off features, which would not be visible in coarser resolution imagery. Consequently, the inundation analysis I completed is closer to representing actual marsh inundation than the same methodology would suggest on coarser resolution satellite data. This is partially because many small die-off

patches would likely miss detection, resulting in the conclusion that the study marsh is under lower levels of flooding stress than it truly is. The differences in these conclusions can carry divergent implications for marsh management. This makes it clear that prioritizing the collection of high-resolution data to map die-off is a promising avenue for improving our understanding of the extent to which SLR impacts this aspect of marshes.

Furthermore, data collected at such high resolutions allows for analyses of spatial variation in continuous data that are not encapsulated at coarser resolutions. For example, with relatively high-resolution satellite DEM data at a 1-meter resolution, a single pixel would hold one elevation value over a square meter of the marsh. With drone data at an 8-centimeter resolution, that same square meter holds approximately 144 pixels, where each pixel holds a unique elevation value for the 8 square centimeters it represents. This increase in resolution better represents the variation in marsh elevation and inherently improves the detail and accuracy of spatial analyses. Moreover, such data quality improvements are a product of technological developments that will only be better utilized as our analytical methodologies continue to evolve.

One such analytical improvement that made this thesis possible is the application of machine learning into land cover mapping. Not only do algorithms speed up analytical processes, but they also allow for the integration of complex decision-making metrics, such as probability density, into the classification decision tree. When modeling complex ecosystems, it is often difficult to reduce their mechanisms to direct, easily digestible relationships without compromising the output's reliability. Applying machine learning in this field provides an avenue for mapping salt marshes in great detail and with ecological accuracy by integrating previously unfeasible complex metrics. Furthermore,

the speed of algorithm processing compared to manual processing allows researchers to try more variations of their analysis in a shorter time frame. This allows researchers, such as the salt marsh UAS group, to run increasingly refined iterations of their code, ultimately producing an output with a higher confidence level in classification accuracy. It also allows researchers to test more hypotheses, or test the same hypothesis in more than one way, further increasing the confidence of their results.

Thanks to the simplicity computer software affords to complex statistical tests, I was able to easily test my elevation data frames by more than one test of difference in RStudio. My base knowledge of statistics was sufficient enough to ensure data robustness under different test conditions, which allowed me to use statistical tools to test my elevation hypothesis in various novel ways that revealed an interesting relationship in the data. Similarly, the increased popularity of open-source software such as RStudio and QGIS enabled me to find multiple forums throughout my analysis that facilitated data troubleshooting. The development of these communities further increases the accessibility of powerful software that can strengthen the analyses of marsh monitoring data.

Future research in this domain can branch off into many unique projects, though they all require prioritization of high-resolution data acquisition. The accessibility and cost-effectiveness of drones in data collection provide the means to do so, and their use should be encouraged in marsh monitoring programs. I emphasize the utility of machine learning in mapping marsh land cover as it provides the means to process large datasets inherent at high temporal and spatial resolutions. Future research, including

work by the salt marsh UAS research group, should focus on improving the accuracy of these models to implement them as a monitoring tool.

I suggest more research is needed in the study of die-off pools as they represent a critical impact of SLR on marsh functionality. This work should aim to identify the mechanisms by which die-off forms, the magnitude of reduction in functionality they support, proper metrics for identification, and possible avenues of intervention. No one project will be able to answer all, if any, of these questions at once, though the publication of all relevant studies will play a crucial role in solving these problems, uncovering evidence-based solutions, and implementing effective salt marsh management.

Bibliography

Cahoon, D. R. 2015. Estimating relative sea-level rise and submergence potential at a coastal wetland. Estuaries and coasts: journal of the Estuarine Research Federation 38:1077–1084.

Fagherazzi, S., G. Mariotti, N. Leonardi, A. Canestrelli, W. Nardin, and W. S. Kearney. 2020. Salt marsh dynamics in a period of accelerated sea level rise. Journal of geophysical research. Earth surface 125.

Farron, S. J., Z. J. Hughes, and D. M. FitzGerald. 2020. Assessing the response of the Great Marsh to sea-level rise: Migration, submersion or survival. Marine geology 425:106195.

FitzGerald, D. M., C. J. Hein, J. E. Connell, Z. J. Hughes, I. Y. Georgiou, and A. B. Novak. 2021, April 15. Largest marsh in New England near a precipice.

FitzGerald, D. M., and Z. Hughes. 2019. Marsh Processes and Their Response to Climate Change and Sea-Level Rise. Annual review of earth and planetary sciences.

Ganju, N. K., Z. Defne, and S. Fagherazzi. 2020. Are elevation and open-water conversion of salt marshes connected? Geophysical research letters 47.

Gustafson, E. J. 2013. When relationships estimated in the past cannot be used to predict the future: using mechanistic models to predict landscape ecological dynamics in a changing world.

Kirwan, M. L., and J. P. Megonigal. 2013. Tidal wetland stability in the face of human impacts and sea-level rise. Nature 504:53–60.

Kirwan, M. L., and A. B. Murray. 2007. A coupled geomorphic and ecological model of tidal marsh evolution. Proceedings of the National Academy of Sciences of the United States of America 104:6118–6122.

Langston, A. K., O. D. Vinent, E. R. Herbert, and M. L. Kirwan. 2020. Modeling long-term salt marsh response to sea level rise in the sediment-deficient Plum Island Estuary, MA.

Leonard, L. A., and A. L. Croft. 2006. The effect of standing biomass on flow velocity and turbulence in Spartina alterniflora canopies. Estuarine, coastal and shelf science 69:325–336.

Morris, J. T., P. V. Sundareshwar, C. T. Nietch, B. Kjerfve, and D. R. Cahoon. 2002. Responses of coastal wetlands to rising sea level. Ecology 83:2869–2877.

Pashaei, M., H. Kamangir, M. J. Starek, and P. Tissot. 2020. Review and Evaluation of Deep Learning Architectures for Efficient Land Cover Mapping with UAS Hyper-Spatial Imagery: A Case Study Over a Wetland. Remote Sensing 12:959.

Payne, A. R., D. M. Burdick, and G. E. Moore. 2019. Potential effects of sea-level rise on salt marsh elevation dynamics in a New Hampshire estuary. Estuaries and coasts: journal of the Estuarine Research Federation 42:1405–1418.

Raposa, K. B., R. L. J. Weber, M. C. Ekberg, and W. Ferguson. 2017. Vegetation dynamics in Rhode Island salt marshes during a period of accelerating sea level rise and extreme sea level events. Estuaries and coasts: journal of the Estuarine Research Federation 40:640–650.

Smith, S. M. 2009. Multi-Decadal Changes in Salt Marshes of Cape Cod, MA: Photographic Analyses of Vegetation Loss, Species Shifts, and Geomorphic Change. Northeastern Naturalist 16:183–208.

Stamp, J., A. Hamilton, M. Liang, J. Clough, M. Propato, L. Haaf, and J. M. West. 2019. Application of the Sea-Level Affecting Marshes Model (SLAMM) to the Lower Delaware Bay, with a Focus on Salt Marsh Habitat. EPA.

Weston, N. B. 2014. Declining sediments and rising seas: An unfortunate convergence for tidal wetlands. Estuaries and coasts: journal of the Estuarine Research Federation 37:1–23.

APPENDIX A: Supplemental Figures

Figure 5: Orthomosaic image of the Red River marsh

Figure 6: Digital Elevation Model (DEM) of the Red River marsh

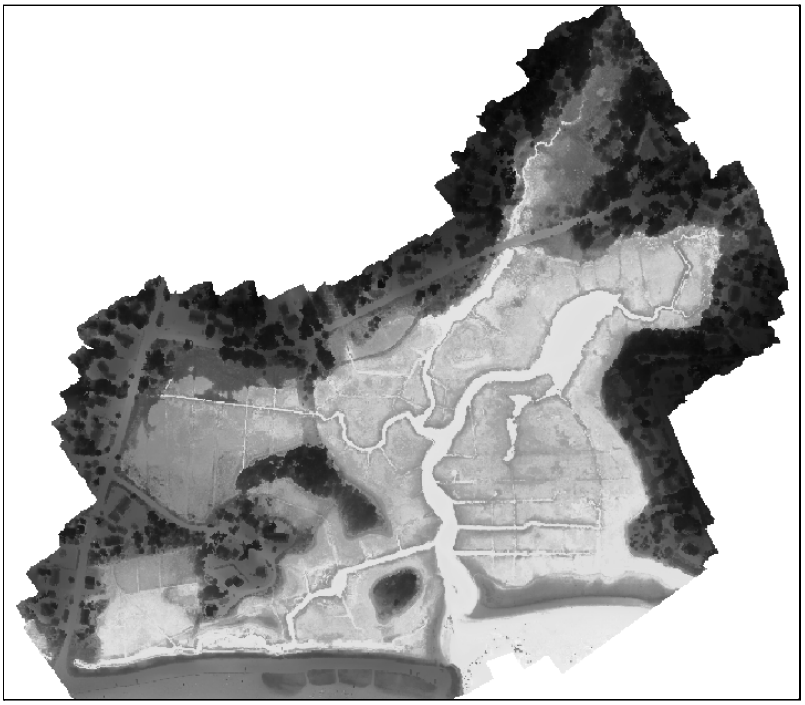

Figure 7: Vegetation (green) and water/bare ground (blue) classification rasters

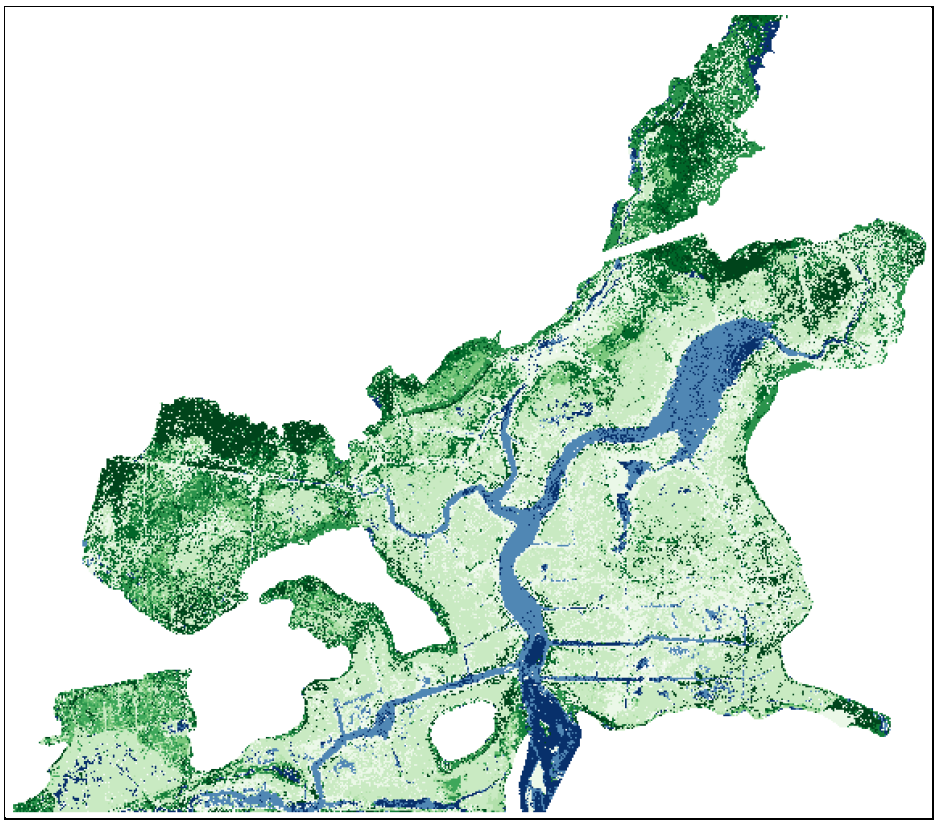

Figure 8: Shifted vegetation raster (green) compared to original vegetation raster (grey)

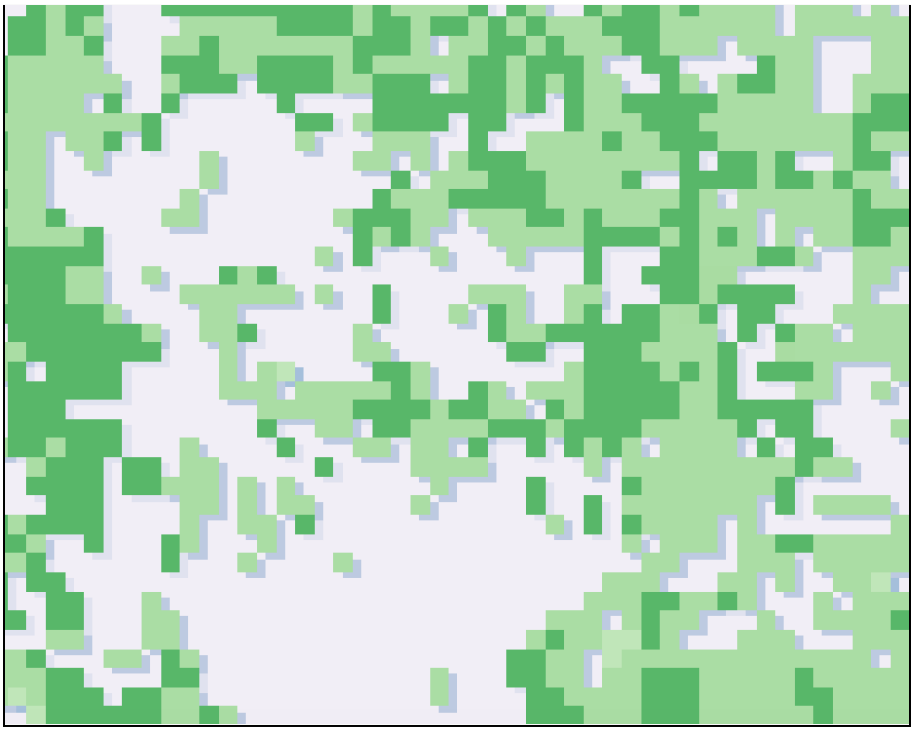

APPENDIX B: Data Tables

Table 1: Highest and lowest running averages of tide levels by month.

Month	Jan	Feb	Mar	Apr	May	Jun	Jul
Spring Tides	0.5517	0.6000	0.6167	0.6267	0.6283	0.6000	0.5783
Neap Tides	0.2633	0.2283	0.2233	0.2833	0.3467	0.3350	0.3267
Month	Aug	Sep	Oct	Nov	Dec	Annual Average	Annual MHT
Spring Tides	0.6450	0.6900	0.6967	0.6667	0.6117	0.6260	0.4466
Neap Tides	0.3183	0.3183	0.3250	0.3400	0.3267	0.3029	

Neap Avg	Critical value	MHT	Critical Value	Spring Avg
0.3029	0.375	0.4466	0.536	0.6260

Table 2: Delta values by land cover subclass

Class	Subclass	Delta value (m)
Vegetation	1	0.3774358344
Vegetation	2	0.2326283321
Vegetation	3	0.2298626244
Vegetation	4	0.1814786072
Vegetation	5	0.3552832251
Vegetation	6	0.179820415
Vegetation	7	0.2436995254
Vegetation	8	0.179324429
Vegetation	9	0.2108446579
Vegetation	10	0.08992824125
Vegetation	11	0.4644785309
Vegetation	12	0.6377645006
Water	22	0.1658532954
Bare ground	31	-0.005431994677
Bare ground	32	0.1874353876
Bare ground	33	0.05904247117